N-glycosyl bonds at the dimer site) which affects the destacking of purines at the dimer site will also affect its binding with photolyase. In fact, Sutherland and coworkers[17] have shown that both the phosphodiester bonds internal to the dimer and the *N*-glycosyl bond joining the pyrimidine base to the deoxyribose must be intact for the *PhrA* photolyase to act. Breaking of either of the above mentioned bonds will remove the constraints imposed by the connectivity via sugar-phosphate backbone. As a consequence, the pyrimidine dimer will become flexible and adjust to a geometry similar to that of the dimerized dimethylthymidine. The structure of DNA under these conditions will be similar to that described by Pearlman *et al.*, which does not predict much destacking of the purines on the complementary strand. Therefore such a nicked DNA will not act as a substrate for the *PhrA* photolyase.

The model proposed above is mainly based on the stacking interactions between a base of RNA cofactor and the destacked target purines, which is essential for the recognition of the dimer site by the photolyase. However, other interactions between photolyase protein and DNA and hydrogen bonding between RNA cofactor and DNA backbone may exist and stabilize the photolyase:UV-irradiated DNA complex.

1. Sutherland, B. M., in *The Enzymes* (ed. Boyer, P. D.), Academic Press, New York, 1981, vol. 17, p. 481.
2. Snapka, R. M. and Sutherland, B. M., *Biochemistry*, 1980, **19**, 4201.
3. Koka, P., *Biochemistry*, 1984, **23**, 2914.
4. Snapka, R. M. and Fuselier, C. O., *Photochem. Photobiol.*, 1977, **25**, 415.
5. Hejmadi, V. S. and Verma, N. C., *Indian J. Biochem. Biophys.*, 1987, **24**, 189.
6. Jones, T. A., *J. Appl. Cryst.*, 1978, **11**, 268.
7. Cadet, J., Voituriez, I., Hruska, F. F. and Grand, A., *Biopolymers*, 1985, **24**, 897.
8. Arnott, S. and Hukins, D. W. I., *Biochem. Biophys. Res. Commun.*, 1972, **47**, 1504.
9. Hermans, J. S. and McQueen, J. F., *Acta. Crystallogr.*, 1974, **A30**, 730.
10. Hendrickson, W. A. and Konnert, J. H., in *Biomolecular Structure, Conformation, Function and Evolution* (ed. Srinivasan, R.), Pergamon Press, Oxford and New York, 1981, vol. I, p. 43.
11. Westhof, F., Dumas, P. and Moras, D., *J. Mol. Biol.*, 1985, **184**, 119.
12. Cimino, G. and Sutherland, J. C., *Biochemistry*, 1982, **21**, 3914.
13. Husain, I., Griffith, J. and Sancar, A., *Proc. Natl. Acad. Sci. USA*, 1988, **85**, 2558.
14. Pearlman, D. A., Holbrook, S. R., Pirkle, D. and Kim, S. H., *Science*, 1985, **227**, 1304.
15. Cameraman, N. and Cameraman, A., *J. Am. Chem. Soc.*, 1970, **92**, 2523.
16. Wun, K. I., Gih, A. and Sutherland, J. C., *Biochemistry*, 1977, **16**, 921.
17. Sutherland, B. M., Oliveira, O. M., Ciarrocchi, G., Brash, D. F., Haseltine, W. A., Lewis, R. I. and Hanawalt, P. C., *Biochemistry*, 1986, **25**, 681.

ACKNOWLEDGEMENTS. We are grateful to Dr B. M. Sutherland for the gift of *E. coli* strain W3350(λcI857S7D→J). We also thank Drs N. K. Notani, R. Chidambaram and K. K. Kannan for their critical comments and suggestions.

15 May 1989; revised 15 November 1989

Genetic variation in some wild populations of *Drosophila busckii*

Ravi Parkash, Jyoutsna and J. P. Yadav
Department of Biosciences, Maharshi Dayanand University, Rohtak 124 001, India

Isofemale lines derived from two natural population samples of *D. busckii* were analysed through horizontal starch gel electrophoresis for genetic variation in nine gene–enzyme systems. Five autosomal loci code for dimeric APH, ODH, MDH, ME and AO phenotypes; as well as allelic variants are represented by segregating single-band variants. Complex ACPH patterns are controlled by a duplicate locus while polymorphic esterase loci code for monomeric enzymes. However, α-GPDH and ADH are controlled by a single locus each and homozygous strains depict epigenetic two-banded phenotypes. Data on genetic structure at sixteen polymorphic loci in two populations of *D. busckii* are discussed here.

ELECTROPHORETIC techniques have revolutionized the status of empirical studies in population genetics, systematics and evolutionary biology[1,2]. Electrophoretic banding patterns can be transformed into allelic and/or non-allelic genetic variations which are used to describe the genetic structure of natural populations[3,4]. Data exist on the extent of genetic variability in local, regional and continental populations of *D. melanogaster* but there is little information on *D. busckii* which is the only known species of the subgenus Dorsilopha[1,5]. The present paper reports the patterns of genic variations occurring at loci coding for glucose-metabolizing enzymes and other enzyme systems in two populations of *D. busckii*.

Methods

D. busckii occurs in nature during December–February. Isofemale lines were established for populations sampled from Rohtak (Haryana) and Chandigarh (Punjab)[6]. Homogenates of single individuals were applied to a 12% horizontal starch gel slab (with a capacity of about 15 samples) and were run electrophoretically at 250 V and 30 mA at 4°C for 4 h. The gel slices were stained for different enzymes[7]. The genetic basis, the nomenclature of banding patterns and the calculation of genetic variability indices were followed from other sources[8–10]. The enzyme abbreviations include: alcohol dehydrogenase (ADH, E.C.1.1.1.1); acid phosphatase (ACPH, E.C.3.1.3.2); alkaline phosphatase (APH, E.C.3.1.3.1.); octanol dehydrogenase (ODH, E.C.1.1.1.73); malate dehydrogenase (MDH, E.C.1.1.1.37); malic enzyme (ME, E.C.1.1.1.40); esterases (Est, E.C.3.1.1.1); α-glycerophosphate dehydrogenase (α-GPDH, E.C.1.1.1.8) and aldehyde oxidase (AO, E.C.1.2.3.1).

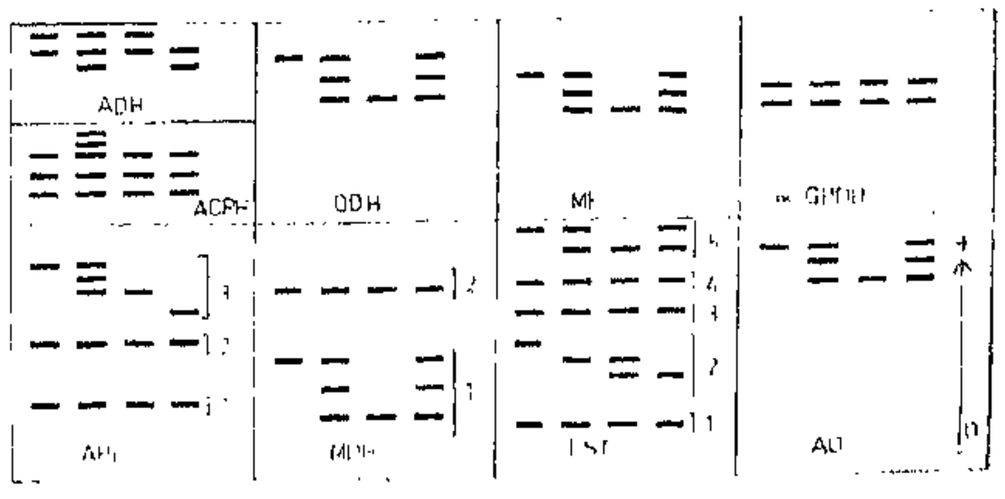

Figure 1. Representation of starch gel electrophoretic patterns for nine gene–enzyme systems in single individual homogenates of *D. busckii*. Multiple zones of activity occur for APH, MDH and EST while all other enzymes are represented by a single zone of activity. Single-band variants and triple-band patterns for APH, ODH, MDH, ME and AO represent homozygous and heterozygous genotypes. Three-banded and five-banded complex ACPH patterns are coded by a duplicate locus. Two-banded α-GPDH patterns are coded by a monomorphic locus. Arrow indicates the direction of current flow.

Results

Electrophoretic phenotypes of nine gene–enzyme systems are represented in Figure 1. Multiple zones of activity

Table 1. Genetic control of electrophoretic phenotypes at polymorphic enzymatic zones in *D. busckii*.

Sl. No.	Zone	Genetic crosses	Enzyme phenotypes FF	FS	SS	Sample size	Testing the Mendelian ratios	χ^{2*}
1.	ACPH	SS × SS	—	—	7	7	—	
		FS × SS	—	8	10	18	1:1	0.22
2.	EST-5	FS × FS	4	7	5	16	1:2:1	0.37
		FS × SS	—	10	12	22	1:1	0.18
		FF × FF	12	—	—	12	—	—
3.	ADH	FS × FS	5	11	8	24	1:2:1	0.91
		SS × SS	—	—	14	14	—	—
		FF × SS	—	30	—	30	—	—
4.	ODH	FF × FF	26	—	—	26	—	—
		FS × SS	—	4	6	10	1:1	0.40
		FS × FF	18	14	—	32	1:1	0.50
5.	MDH-1	FF × FS	14	16	—	30	1:1	0.13
		FS × FS	7	18	11	36	1:2:1	0.88
		SS × FS	—	8	12	20	1:1	0.80
6.	ME	FF × FS	3	5	—	8	1:1	0.50
		FS × FS	4	9	3	16	1:1	0.37
		SS × SS	—	—	15	15	—	—

Sl. No.	Zone	Genetic crosses	FF	MM	SS	FM	FS	MS	Sample size	Testing the Mendelian ratios	χ^{2*}
7.	EST-2	FF × MM	—	—	—	17	—	—	17	—	—
		MS × MS	—	8	10	—	—	22	40	1:2:1	0.60
		FS × FS	4	—	8	—	12	—	24	1:2:1	1.32
		MM × FM	—	8	—	10	—	—	18	1:1	0.22
8.	APH-3	SS × FM	—	—	—	—	14	18	32	1:1	0.50
		SS × MS	—	—	9	—	—	11	20	1:1	0.20
		FM × FM	3	4	—	5	—	—	12	1:1	0.49
		MM × SS	—	—	—	—	—	9	9	—	—
9.	AO	FF × SS	—	—	—	—	17	—	17	—	—
		FS × FS	3	—	5	—	8	—	16	1:2:1	0.50
		FS × SS	—	—	4	—	6	—	10	1:1	0.40

*Non significant at 5% level. Sl. no. 1 to 6 represent diallelic loci while Sl. no. 7 to 9 refer to triallelic loci. F, M, S represent fast, medium and slow segregating electrophoretic variants (allozymes); FF, MM and SS refer homozygous genotypes while FS, MS and FS represent heterozygous genotypes.

occur for three enzymes (APH, MDH and EST) while all other enzymes are represented by a single zone. The banding patterns at different zones are independent of each other. Gel slices stained for esterases revealed five zones of activity. The EST-2 and EST-5 zones are represented by segregating single-band variants and two-band patterns while other non-segregating EST zones are monomorphic. Genetic crosses revealed that segregation patterns of esterase bands at polymorphic zones agree with monogenic inheritance (Table 1). However, a single polymorphic zone each for AO, ODH, MDH-1, ME and APH-3 is represented by segregating single-band variants and three-band patterns. Genetic crosses between individuals with triple-band and single-band patterns produced about equal proportions of offsprings with electrophoretic phenotypes like the parents. Thus the segregation ratios of electrophoretic phenotypes for these enzymes were found to agree with monogenic Mendelian inheritance (Table 1). The banding patterns did not vary with sex and thus the enzyme phenotypes are coded by distinct autosomal loci. The single-band variants and triple-band patterns at each segregating zone represent homozygous and heterozygous genotypes respectively and such enzymes are dimeric in nature.

Complex ACPH patterns in *D. busckii* include three-banded and five-banded patterns. ACPH being dimeric molecules, the occurrence of triple-banded patterns in long term in-bred laboratory strains could only be interpreted on the basis of a duplicate locus. However, this suggestion needs to be verified by dissociation–reassociation of ACPH isozymes. A single monomorphic zone of α-GPDH is represented by two-banded patterns while the single ADH zone depicted segregating patterns of two-banded and three-banded phenotypes in single individuals. Genetic crosses involving different two-banded ADH patterns resulted in three-banded patterns in F_1 and a segregation ratio of 1:2:1 in F_2 (Table 1). Thus, ADH and α-GPDH constitute conformational electrophoretic phenotypes and are under the independent control of a single locus each.

The data on distribution of genotypes, allelic frequencies, the observed and expected heterozygosity, Wright's fixation index (f) and log-likelihood χ^2 test for fit to Hardy–Weinberg expectations at nine polymorphic loci

Table 2. Data on distribution of observed and expected genotypes, allelic frequencies, heterozygosity, effective number of alleles (n_e), Wright's inbreeding coefficient (f) and G-values for log-likelihood χ^2 test for fit to Hardy–Weinberg expectations at six loci in two natural populations of *D. busckii*.

Locus	Populations	Genotypes FF	Genotypes FS	Genotypes SS	Sample size	Allelic Freq. F	Allelic Freq. S	Heterozygosity Obs./Exp.	n_e	$f \pm$ S.E.	G-values
ACPH	CHD	0 (0.53)	18 (16.47)	128 (129)	146	0.06	0.94	0.123/0.113	1.13	−0.09 ± 0.01	1.20
	RTK	0 (1.25)	23 (20.17)	80 (81.58)	103	0.11	0.89	0.223/0.196	1.24	−0.14 ± 0.02	2.91
EST-5	CHD	20 (19.03)	44 (46.53)	30 (28.44)	94	0.45	0.55	0.468/0.495	1.98	0.05 ± 0.01	0.27
	RTK	18 (17.42)	44 (44.35)	28 (28.22)	90	0.44	0.56	0.488/0.493	1.97	0.01 ± 0.00	0.04
ADH	CHD	4 (0.51)	6 (13.54)	94 (89.95)	104	0.07	0.93	0.057/0.130	1.15	0.56 ± 0.03	14.99*
	RTK	4 (0.36)	4 (11.28)	92 (88.36)	100	0.06	0.94	0.04/0.113	1.13	0.64 ± 0.03	18.39*
ODH	CHD	14 (11.56)	40 (44.88)	46 (43.56)	100	0.34	0.66	0.40/0.45	1.81	0.11 ± 0.02	1.17
	RTK	10 (11.26)	50 (45.87)	50 (50.86)	110	0.32	0.68	0.454/0.435	1.77	−0.04 ± 0.01	0.27
MDH-1	CHD	58 (53.25)	50 (59.90)	22 (16.85)	130	0.64	0.36	0.384/0.461	1.85	0.17 ± 0.02	3.58
	RTK	40 (36.72)	42 (48.96)	20 (16.32)	102	0.60	0.40	0.412/0.48	1.92	0.14 ± 0.02	2.09
ME	CHD	8 (6.22)	32 (35.40)	52 (50.38)	92	0.26	0.74	0.348/0.385	1.62	0.09 ± 0.02	0.85
	RTK	16 (12.74)	40 (47.32)	48 (43.94)	104	0.35	0.65	0.384/0.455	1.83	0.15 ± 0.02	2.33

*Significant at 5% level; all other values are non-significant. F and S represent allelic isozymes (allozymes/electromorphs). FF and SS refer to genotypes homozygous for fast (F) and slow (S) allelic variants while FS refers to heterozygous genotypes. The numbers in parentheses refer to expected number of genotypes, (Exp. het. $= 1 - \Sigma x_i^2$); $n_e = 1/\Sigma x_i^2$; $f = (1 - \text{obs. het/exp. het.})$. S.E. = Standard error.
CHD, Chandigarh; RTK, Rohtak.

Table 3. Data on distribution of observed and expected genotypes, allelic frequencies, heterozygosities, effective number of alleles (n_e), Wright's inbreeding coefficient (f) and G-values for log-likelihood χ^2 test for fit to Hardy–Weinberg expectations at three loci in two natural populations of *D. busckii*

Locus	Populations	Genotypes FF	MM	SS	FM	FS	MS	Sample size	Allelic Freq. F	M	S	Het. Obs./Exp.	n_e	f ± S.E.	G-values
EST-2	CHD	6 (5.70)	27 (21.87)	9 (8.33)	18 (22.33)	18 (13.78)	21 (26.99)	99	0.24	0.47	0.29	0.57/0.64	2.75	0.10 ± 0.02	4.70
	RTK	9 (10.38)	24 (17.28)	12 (9.08)	24 (26.78)	24 (19.42)	15 (25.06)	108	0.31	0.40	0.29	0.58/0.64	2.78	0.09 ± 0.02	9.39*
APH-3	CHD	0 (1.47)	6 (12.49)	30 (28.65)	18 (8.57)	6 (12.97)	42 (37.84)	102	0.12	0.35	0.53	0.65/0.58	2.39	−0.11 ± 0.02	20.19*
	RTK	2 (1.50)	4 (10.29)	26 (25)	15 (7.87)	4 (12.26)	38 (32.08)	89	0.13	0.34	0.53	0.64/0.59	2.42	−0.09 ± 0.02	18.89*
AO	CHD	28 (31.37)	0 (0.10)	24 (23.49)	8 (3.62)	56 (54.29)	0 (3.13)	116	0.52	0.03	0.45	0.55/0.53	2.11	−0.05 ± 0.01	10.83*
	RTK	28 (28.57)	—	32 (33.53)	—	64 (61.90)	—	124	0.48	—	0.52	0.52/0.50	2.0	−0.03 ± 0.01	0.15

F, M and S represent allelic isozymes (allozymes/electromorphs). FF, MM and SS represent genotypes homozygous for fast (F), medium (M) and slow (S) allelic variants while FM, MS and FS represent heterozygous genotypes. Number in parentheses refer to expected number of genotypes. Exp. het. $= 1 - \Sigma x_i^2$; $n_e = 1/\Sigma_i^2$; $f = (1 - \text{obs. het./exp. het.})$. *Significant at 5% level; other values are non-significant. The positive and negative values of Wright's fixation index (f) indicate deficiency of heterozygotes and excess of heterozygotes respectively. CHD, Chandigarh; RTK, Rohtak. (Chandigarh: 30.43 N and 76.54 E; Rohtak: 28.94 N and 76.38 E).

in *D. busckii* are given in Tables 2 and 3. Data on genetic indices (number of alleles, allelic frequencies and heterozygosity) for diallelic loci (ACPH, EST-5, ADH, ODH, MDH-1, ME) and triallelic loci (EST-2, APH-3 and AO) have revealed similarity in genic diversity patterns in two natural populations of *D. busckii* (Tables 2 and 3). *D. busckii* populations are characterized by high heterozygosity at most of the polymorphic loci; and the range of heterozygosities observed at the various loci correlates well with the incidence of number of alleles as well as allelic frequencies distribution patterns. The higher values of f at ADH locus in both populations indicate significant deficiency of heterozygous genotypes at this locus. The population samples of *D. busckii* have shown deviations from Hardy–Weinberg expectations at ADH, EST-2, APH-3 and AO loci out of sixteen loci analysed.

Discussion

A locus is considered polymorphic if the frequency of the most common allele does not exceed 0.99; accordingly all the nine loci in *D. busckii* populations examined are polymorphic[1,2]. The different gene–enzyme systems in *D. busckii* have revealed contrasting patterns of electrophoretic phenotypes. The occurrence of two-banded electrophoretic phenotypes of ADH and α-GPDH in homozygous strains of *D. busckii* significantly differs from the single-banded phenotypes (in case of APH-3, EST-2, EST-5, AO, ODH, MDH-1, ME) which represent allelic isozymes (allozymes). The present observations on ADH and α-GPDH concur with other reports that in NAD requiring dehydrogenases, more than one electromorph (conformational isozyme) may arise due to post-translational differential binding of coenzyme NAD[11–13].

Previous electrophoretic data on *D. busckii* are limited to a single study which revealed low amount of genic variation (i.e. $P = 0.166$ and $H = 0.044$) in laboratory maintained stocks of US populations of this species[5] (Table 4). The present observations on the extent of polymorphic loci ($P = 0.56$ for both populations), allelic frequencies; and heterozygosity ($H_o/H_e =$ 0.222/0.236 for Chandigarh (CHD) population and 0.234/0.244 for Rohtak population) in *D. busckii* from northern India differ significantly from those on US populations (Table 4). The low amount of genic variation ($H = 0.044$) reported for US laboratory populations of *D. busckii* could be due to extensive inbreeding in 2–10 year old cultures as well as operation of genetic drift resulting in fixation of alleles at most loci.

The mechanism for the maintenance of genetic polymorphism has been argued on the basis of selectionist or neutralist hypotheses[14–17]. According to neutralist, the patterns of random genetic differences between populations are expected while occurrence of

Table 4. Data on genetic indices in *D. busckii* populations.

Genetic indices	Populations Chandigarh	Rohtak
No. of loci examined	16	16
Average no. of alleles/locus	1.75	1.687
Proportion of polymorphic loci (P)	0.56	0.56
Heterozygosity (observed) H_o	0.222	0.234
Heterozygosity (expected) H_e	0.236	0.244

In US popultion of *D. busckii*, $P = 0.166$ and $H = 0.044$ (c.f. ref. 5).

uniformity has been taken as evidence of operation of some type of natural selection. The present study revealed similar patterns of genic variation at nine polymorphic loci in two natural populations of *D. busckii* and this could be interpreted due to action of some type of natural selection (Tables 2–4). The present studies need to be extended to several ecogeographical populations of *D. busckii* to assess the extent of genetic variability in this species compared to the other colonizing *Drosophila* species.

1. Wills, C., *Genetic Variability*, Clarendon Press, Oxford, 1981.
2. Milkman, R., *Perspectives in Evolution*, Sinauer Associates, Inc., Champaign, 1982.
3. MacIntyre, R. J., *Molecular Evolutionary Genetics*, Plenum, New York, 1986.
4. Parkash, R., *Ind. Rev. Life Sci.*, 1987, **7**, 141.
5. Prakash, S., *Genetics*, 1973, **75**, 571.
6. Parsons, P. A., *Evol. Biol.*, 1980, **13**, 175.
7. Harris, H. and Hopkinson, D. A., *Handbook of Enzyme Electrophoresis in Human Genetics*, North-Holland, Amsterdam, 1976.
8. Dickinson, W. J. and Sullivan, D. T., *Gene Enzyme Systems in Drosophila*, Springer-Verlag, Berlin, 1975.
9. Fergusson, A., *Biochemical Systematics and Evolution*, Wiley, New York, 1980.
10. Zar, J. H., *Biostatistical Analysis*, Prentice-Hall, Englewood, New Jersey, 1984.
11. O'Brien, S. J. and MacIntyre, R. J., in *Genetics and Biology of Drosophila* (eds Ashburner, M. and Wright, T.), Academic Press, London, 1978, vol. 2a, p. 396.
12. Gillespie, J. H. and Kojima, K., *Proc. Natl. Acad. Sci. USA*, 1966, **61**, 582.
13. Johnson, G. B., *Science*, 1974, **184**, 28.
14. Hedrick, P. W., *Genetics of Populations*, Science Books International, Boston, 1983.
15. Karlin, S. and Nevo, E., *Evolutionary Processes and Theory*, Academic Press, New York, 1986.
16. Girard, P., Palabost, L. and Petit, C., *Biochem. Genet.*, 1977, **15**, 589.
17. Singh, R. S., Hickey, D. A. and David, J. R., *Genetics*, 1982, **101**, 235.

ACKNOWLEDGEMENTS. Financial assistance from CSIR, New Delhi, is gratefully acknowledged. J. P. Yadav thanks UGC, New Delhi for a fellowship. We are grateful to the reviewer for several helpful suggestions.

21 March 1989; revised 15 November 1989

Gasket-compression mechanism of pressure-pulse generation by low-velocity projectile impact on opposed anvil set-up

A. K. Singh
Materials Science Division, National Aeronautical Laboratory, Bangalore 560 017, India

High pressure pulse is generated when a low-velocity projectile strikes a tungsten carbide opposed anvil system with pyrophyllite gasket and solid pressure transmitting medium. A possible mechanism based on the gasket-compression is proposed for generation of such pressure pulses.

IT has been shown recently[1] that a high pressure pulse of short duration is produced in the gasket region when a low-velocity projectile strikes a tungsten carbide-opposed anvil set-up with pyrophyllite gasket and solid pressure transmitting medium. Both the amplitude and the duration of the pressure pulse depend upon the momentum of the projectile. The experiments with anvils of 12 mm diameter face indicate that the amplitude of the pressure pulse increases from 2 to 6 GPa and the pulse duration from 280 to 380 μs as the momentum of the projectile (mass in the range of 5–10 kg) is increased from 10 to 60 kg m s^{-1}.

The pressure versus time data representing a typical pressure pulse as derived from the resistance-time data of a manganin gauge, are shown in Figure 1. Except in the small regions near the start and the peak of the pressure pulse, the pressure is found to increase linearly with time, the nonlinearity being $<5\%$. The rate of pressure increase can be varied between 0.03 and

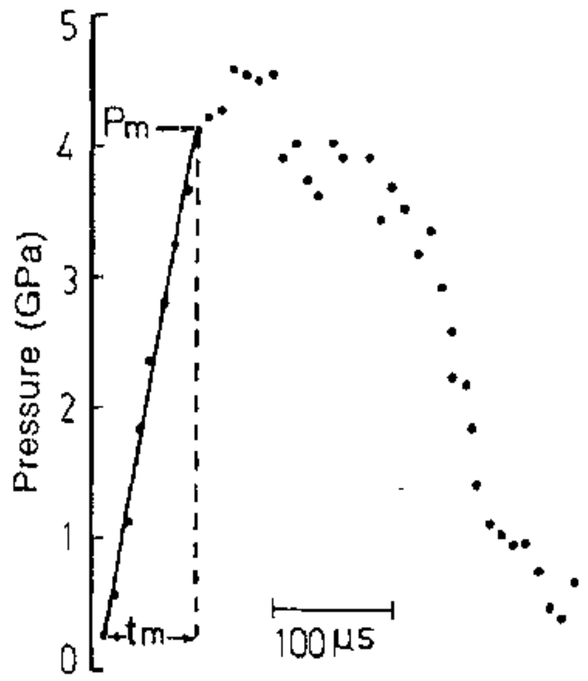

Figure 1. A typical pressure pulse obtained under impact loading. P_m is the maximum pressure up to which the pressure increase is linear. The peak pressure is 10–15% higher than P_m.